

ARTICLE

Effect of Thermal Treatment on the Catalytic Performance of Magnesium Oxide-Hydroxide Systems in Biodiesel Production from Jatropha Oil: Homogeneous versus Heterogeneous Catalytic Action**Hamzeh Telfah, Sabri Mahmoud and Ayman Hammoudeh****Chemistry Department, Yarmouk University, Irbid-Jordan.**Received on: 30th Jan. 2018;**Accepted on: 10th Apr. 2018*

Abstract: A series of magnesium oxide-hydroxide catalysts was prepared and tested for their efficiency in catalyzing the transesterification of raw Jatropha oil into biodiesel. Thermal treatment was found to play a crucial role in determining the catalytic activity and calcination of Mg(OH)₂ for two hours at 350°C was found to give mixed Mg(OH)₂ and MgO phases with high activity as rather small amounts of this catalyst (only 0.25 g per 20 g oil) could achieve in three hours of transesterification with methanol at 60°C a conversion of 75%. The solubility of the above system in methanol was determined to be 1.53×10^{-4} M, suggesting that its catalytic action is both of homogenous (dissolved hydroxide ions) as well as of heterogeneous (basic surface sites) nature. Thermal treatment at 500°C results in a less active system (biodiesel yield 47%) which could be related to decreased amount of soluble fraction (solubility in methanol 6.7×10^{-5} M) and to decreased strength of basic surface sites as suggested by the CO₂ desorption experiments. Nevertheless, the system resulting from the thermal treatment at 500°C is believed to be the better one in terms of heterogeneity and thus recyclability; higher amounts must however be used for longer periods of time in order to achieve higher yields.

Keywords: Biodiesel, Jatropha, Heterogeneous catalysis, MgO.

Introduction

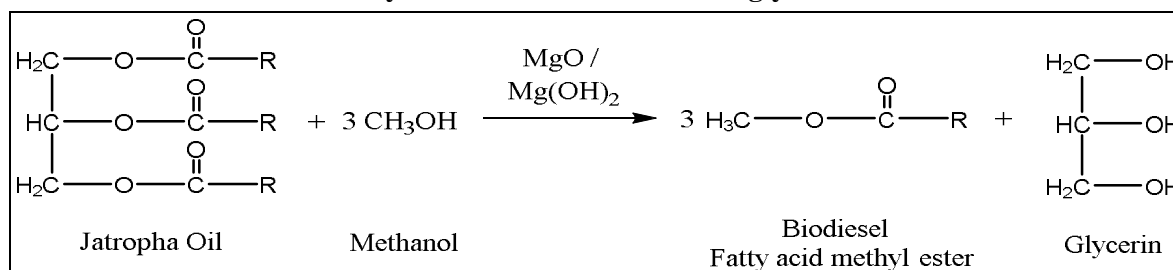
The commercial production of biodiesel and its application as a substitute for petroleum diesel grew largely in the past decades and an almost 47-fold increase in the global annual production has been witnessed in the period from 2000 to 2013^[1]. The main advantages of biodiesel is its renewability, biodegradability, reduced CO₂ emissions and reduced harmful gas emissions, such as SO₂^[2-4]. Conventional industrial processes are however based on the application of homogeneous catalysts (e.g. potassium hydroxide and sodium hydroxide) for the transesterification reaction of oils/fats with methanol or ethanol (Scheme 1)^[5]. In addition to the rather high washing and separation requirements associated with the application of homogeneous catalysts, these catalysts are hygroscopic, caustic and end up polluting the

environment^[6]. In addition, a major disadvantage of biodiesel production lies in the fact that it is based mostly on edible vegetable oils as raw material, which leads in turn to the so-called food-fuel competition that drives the oil prices high and rises doubts with respect to the sustainable use of these raw materials in the long term^[7]. A reasonable solution would be to replace edible vegetable oils with oils that can be produced from drought/salt tolerant non-food plants grown on low-quality arid lands and irrigated by low-quality water. With this respect, Jatropha seems to be a good choice, since its oil is inedible and Jatropha trees can withstand dryness and very poor soil and can also grow in saline conditions^[8].

Moreover, it is easy to establish; it grows relatively quickly and lives producing seeds for 50 years^[9]. In 2005, *Jatropha curcas* seeds were introduced in Jordan from India and grown under

saline water irrigation and under reclaimed wastewater for research purposes on biodiesel production^[10].

Scheme 1. Base catalyzed transesterification of triglycerides with methanol.



Aiming at reducing the separation costs as well as the negative environmental impact associated with the application of conventional homogenous base catalysts, research activity has been intensified on the search for solid catalysts; a wide variety of solid systems have been tested for this purpose with a lot of attention devoted to earth alkaline metal oxides in virtue of their high activity. With this respect, various forms of magnesium oxide systems were studied. A 90% conversion has been reported to be achieved within one hour of reaction at 180°C using a 5% MgO loading and a 12:1 methanol-to-oil molar ratio^[11]. Li₂O-doped MgO produced high biodiesel yield (93.9%) within two hours at 333 K; metal leaching was however significant^[12]. To reduce leaching, TiO₂-MgO mixed oxides were prepared which achieved lower Mg and Ti leaching of 19 and 7 ppm, but the reaction temperature was as high as 423 K with a low biodiesel yield of 79.9%^[13]. A MgO-Li₂O catalyst templated by PDMS-PEO copolymer (poly(dimethylsiloxane-ethylene oxide)) as a structure-directing agent has been investigated; Li/Mg molar ratio of 0.12 and calcination at 873 K produced a catalyst with 90% biodiesel production and minimum leaching after 6 hours of reaction at 333 K with a methanol-to-oil molar ratio of 30^[14]. The basic strength of the MgO-Li₂O catalysts was thereby reported to be enhanced due to the lattice distortion and defects created by the substitution of the Li ions in the MgO lattice^[14]. MgO prepared by metal-chitosan complexation method showed a higher biodiesel production in the transesterification of soybean oil compared to commercial MgO, but the catalyst was susceptible to poisoning and deactivation due to contact with CO₂ and H₂O present in the ambient air^[15]. CaO/MgO catalysts obtained by the thermal treatment of natural dolomite were applied in the microwave-

assisted transesterification of *Jatropha curcas* oil with methanol and conversions reaching 96% (methanol-to-oil molar ratio of 18, 4% catalyst loading) were reported^[16]. The effect of calcination temperature on the activity of MgO nano-particles prepared by the hydration-dehydration method in the transesterification of palm oil with methanol was described by Yacob et al, where a maximum conversion of only 51.3% has been achieved after calcination at 600°C^[17]. To date, it is still a challenge to find an active and stable solid catalyst, which could give high yields of biodiesel under mild reaction conditions (low temperature and pressure). In this paper, the effect of thermal treatment on the catalytic performance of solid magnesium oxide-hydroxide (MgO/Mg(OH)₂) systems in the transesterification of *Jatropha* oil is addressed, with special focus on the question of the nature of the catalytic species in action.

Experimental

Jatropha Oil: Extraction and Analysis

Jatropha fruits were obtained from the National Center for Agricultural Research and Extension (NCARE) in Jordan. The fruits were peeled off to obtain the seeds, which were found to constitute ~ 60% of the fruit mass. n-hexane was added to the finely ground *Jatropha* seeds (1 L hexane/1 kg seeds); the obtained slurry was mixed at 2500 rpm for 1 h at room temperature and the liquid phase was separated by suction filtration. Hexane was removed by rotary evaporation (Büchi Rota evaporator R110) and the remaining *Jatropha* oil was found to constitute about 20% w/w of the seeds. The acidity of the *Jatropha* oil was less than 0.40%; further characteristics, including the fatty acid profile, can be found in^[18].

Catalysts

The magnesium oxide-hydroxide catalysts were prepared by adding a small excess of KOH to an aqueous solution of magnesium nitrate hexahydrate (BDH Chemicals, Ltd.). The precipitated magnesium hydroxide was centrifuged and washed with water until the washing water became neutral. The white gel (magnesium hydroxide) was dried at 120°C, powdered and then subjected to thermal treatment for two hours under flowing oxygen at 250°C, 350°C or 500°C. The resulting systems (designated as Mg(OH)₂/MgO-120, Mg(OH)₂/MgO-250, Mg(OH)₂/MgO-350, Mg(OH)₂/MgO-500, respectively) were characterized with respect to their structure by means of X-ray diffraction (XRD) using a Shimadzu XRD-6000 LabX device with a Cu-K_α-tube ($\lambda = 1.5418 \text{ \AA}$). The functional groups were monitored by infrared spectroscopy (ATR-FTIR) using a Bruker Tensor-27. The surface basic character was evaluated by CO₂ chemisorption applying a pulse flowing technique, where 0.20 g of the prepared catalyst was placed in the center of a tubular pyrex reactor (6 mm id \times 20 cm L) heated under helium for 20 min at the temperature at which it was prepared. The catalyst was then allowed to cool down to 20°C and 250 μ l pulses of CO₂ were then injected into the reactor. If injected CO₂ is chemisorbed, then no CO₂ will reach the thermal conductivity detector (TCD) and no change of the detector signal is observed. When the surface, however, becomes saturated with CO₂, the CO₂ injected passes over the catalyst unaffected and reaches the detector producing a signal. From the number of the CO₂ injections missing at the detector, the total amount of chemisorbed CO₂ can be determined and the number of basic centers at the catalyst surface can be evaluated. The strength of chemisorption was determined by means of Thermal Desorption Spectroscopy (TDS), in which CO₂ on the surface is desorbed by increasing the temperature of the catalyst linearly (i.e., with a constant heating rate). Desorbed CO₂ is detected by the TCD as a function of the catalyst temperature.

Biodiesel Production

Preesterification

In a 100 ml round bottom flask, 25 g of oil

were refluxed with methanol (5% w/w methanol/oil ratio) and concentrated sulfuric acid (1% w/w acid/oil ratio) for two hours. The acid value of resulting oil was determined after washing with water and drying with anhydrous Na₂SO₄ by titration with ethanolic KOH solution according to standard methods^[19].

Transesterification

Homogeneously base-catalyzed transesterification with methanol (6:1 methanol/oil mole ratio) was carried out for 3 h at 60°C using KOH (1.2% w/w KOH/Methanol ratio) as a catalyst. The reaction progress was monitored by ¹H-NMR (Bruker Avance 300) after washing with water and drying up with anhydrous Na₂SO₄. In the case of the heterogeneously base-catalyzed transesterification, the reaction was carried out as described above; KOH was replaced by 0.5 g of the solid base per 40 g oil.

Extractive Transesterification

In this method, both extraction of the oil from the seeds and its subsequent transesterification are carried out simultaneously in one step. The effectiveness of a variety of catalysts (H₂SO₄, MgO/Mg(OH)₂-350 and KOH, in this process was investigated. 20 grams of *Jatropha* seeds were finely ground, then loaded into a 250 ml round bottom flask and mixed with 4.0 g catalyst and 210 ml methanol. The flask was then equipped with a reflux condenser and the temperature held constant at 60°C. The reaction was allowed to proceed for 15 hours; a sample of oil was taken at the end of the reaction. The samples were analyzed by ¹H-NMR.

Results and Discussion

Catalysts Characterization

X-ray Diffraction (XRD)

Figure 1 represents the X-ray diffraction patterns of the various MgO/Mg(OH)₂ systems investigated in this work. Mg(OH)₂ is characterized by the diffraction lines at $2\theta = 32.76^\circ$, 37.86° , 50.66° , 58.50° , 62.0° and 68.22° , which agree with those of the reference pattern of Mg(OH)₂ (JCPDS 00-007-0239). There are, however, rather small diffraction features that are still not identified; for example, those at 34.01° , 45.48° and 55.45° (assigned by asterisk in Figure 1). These can in principle be associated with several complex phases that can

also be present such as mixed magnesium hydroxide/carbonate of various stoichiometries as well as magnesium hydroxide/nitrate. The diffraction lines of $\text{Mg}(\text{OH})_2$ observed in Figure 1 are rather broad. Line broadening in XRD takes place as a result of having a particle size below 100 nm and/or due to deviation from perfect crystallinity.

The relative intensity of the diffraction lines of $\text{Mg}(\text{OH})_2$ was found to decrease as the temperature is increased at which the thermal treatment is performed. New diffraction features appear thereby at 42.78° , 74.49° and 78.51° ,

indicating the formation of MgO as suggested by comparison with the reference pattern of MgO (JCPDS 00-004-0829). Thermal treatment at 500°C causes the major diffraction lines corresponding to $\text{Mg}(\text{OH})_2$ to disappear completely while those of MgO become dominant (small unidentified lines assigned by asterisk in Figure 1 are still observed). It can thus be concluded that the formation of almost phase pure MgO did take place only in this thermal treatment at 500°C . It is however still not perfectly crystalline as can be concluded from the rather large line broadening.

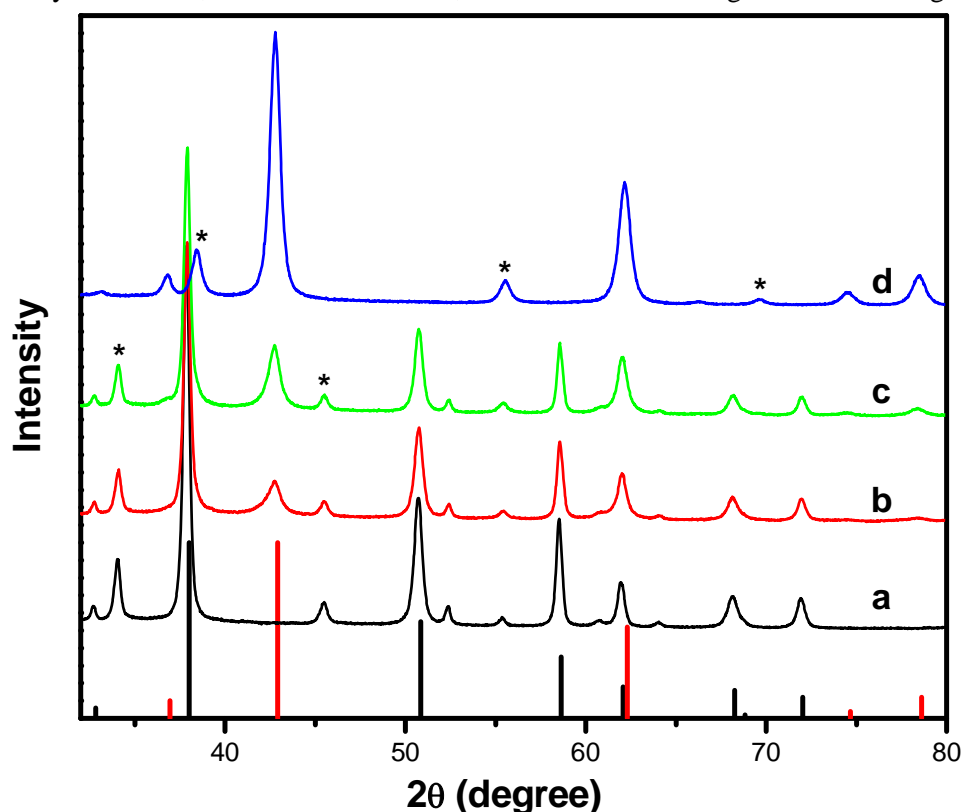


Figure 1. XRD Diffraction patterns of the $\text{MgO-Mg}(\text{OH})_2$ systems; thermal treatment at a) 120°C , b) 250°C , c) 350°C and d) 500°C . Reference stick patterns for $\text{Mg}(\text{OH})_2$ (black) and MgO (red) are included as vertical lines.

Surface Basicity

Figure 2 represents the destiny of CO_2 (Lewis acid) pulses injected over $\text{Mg}(\text{OH})_2/\text{MgO-500}$ at 20°C . The first two injections are completely missing at the detector, indicating that they have been adsorbed by the basic centers at the $\text{MgO-Mg}(\text{OH})_2$ surface. With increasing number of injections, the amount of CO_2 (i.e., peak area) appearing at the TCD detector becomes larger and larger, apparently due to the fact that the surface becomes gradually saturated with CO_2 . When the surface becomes completely saturated

with CO_2 , no change of the CO_2 signal intensities at the detector is observed (last two injections in Figure 2a). Basicity determination was carried out for $\text{Mg}(\text{OH})_2/\text{MgO-350}$ and $\text{Mg}(\text{OH})_2/\text{MgO-500}$ by calculating the area of CO_2 injections missing at the detector and correlating this area with that of a single CO_2 injection. Knowing that each CO_2 injection has a volume of $250\ \mu\text{L}$, the total volume of CO_2 adsorbed at 20°C was determined to be $\sim 3160\ \mu\text{L}\ \text{CO}_2/\text{g}\ \text{Mg}(\text{OH})_2\text{-MgO}$ in both cases. This corresponds to $\sim 13.1\ \text{mmol}$ of basic centers per gram $\text{MgO-Mg}(\text{OH})_2$.

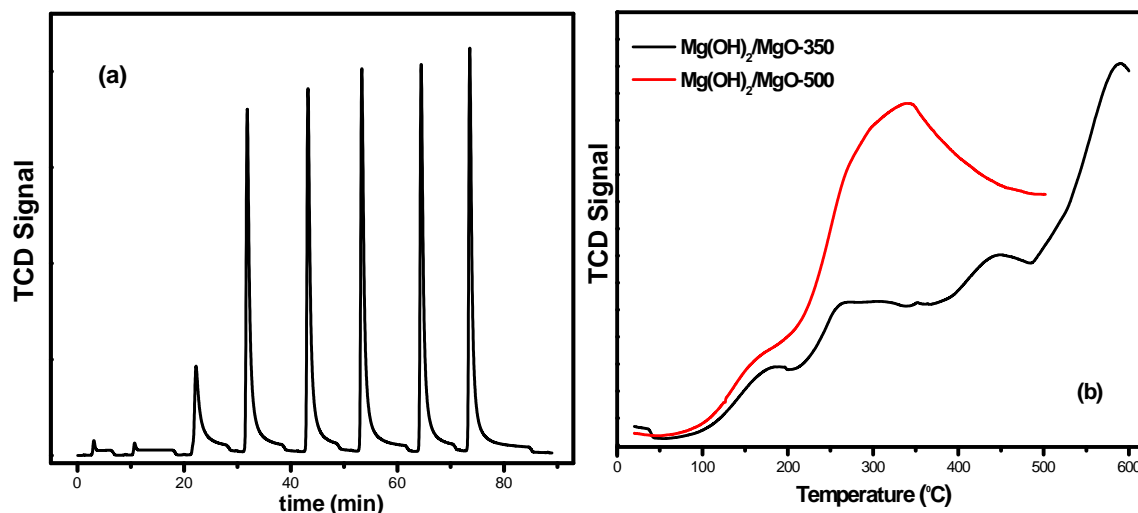


Figure 2. a) CO_2 chemisorption onto MgO-500 at 20°C via the pulse technique, b) Thermal desorption spectra of CO_2 chemisorbed on $\text{Mg(OH)}_2/\text{MgO-350}$ and $\text{Mg(OH)}_2/\text{MgO-500}$.

The thermal desorption spectra (TDS) of CO_2 chemisorbed on $\text{Mg(OH)}_2/\text{MgO-350}$ and $\text{Mg(OH)}_2/\text{MgO-500}$ are shown in Figure 2b. Although both systems have the same concentration of basic centers, they differ significantly in the strength of these basic centers. In the case of $\text{Mg(OH)}_2/\text{MgO-500}$, CO_2 desorbs at much lower temperatures than in the case of $\text{Mg(OH)}_2/\text{MgO-350}$, indicating that in the latter, CO_2 is more strongly adsorbed to the surface, which means in turn that the corresponding basic centers that “captured” the CO_2 molecule are stronger in basicity compared to those in $\text{Mg(OH)}_2/\text{MgO-500}$. The nature of the basic centers onto which CO_2 chemisorbs was not investigated further. It is however known that CO_2 adsorbs both on basic oxygen atoms at the metal oxide surface as well as on basic hydroxyl groups, leading to the formation of carbonate and hydrogen carbonate species, respectively. The hydroxyl groups can be identified by IR spectroscopy and Figure 3 shows a rather sharp O-H stretching band for the

various $\text{Mg(OH)}_2/\text{MgO}$ systems investigated in this work appearing at 3694 cm^{-1} . The position of this band suggests that it belongs most probably to type II and type III surface hydroxyl groups, where the oxygen atom of the hydroxyl group is bonded to two or three metal ions, respectively. In the case of Al_2O_3 , type II and type III hydroxyl groups were reported to appear in the ranges $3730\text{--}3745\text{ cm}^{-1}$ and $3685\text{--}3705\text{ cm}^{-1}$, respectively^[20]. Due to the smaller charge on Mg, the O-H bond is however expected to be less polarized than in the case of Al_2O_3 , the reason why this band is expected to appear slightly shifted to smaller wave numbers. Figure 4 shows that the intensity of this band decreases with increased temperature of the thermal treatment in agreement with the XRD results that show decreased amounts of Mg(OH)_2 at higher temperatures. The stronger basic centers observed in the case of $\text{Mg(OH)}_2/\text{MgO-500}$ (Figure 2b) are therefore attributed to the oxide species at the surface formed as a result of surface dehydroxylation at higher temperatures.

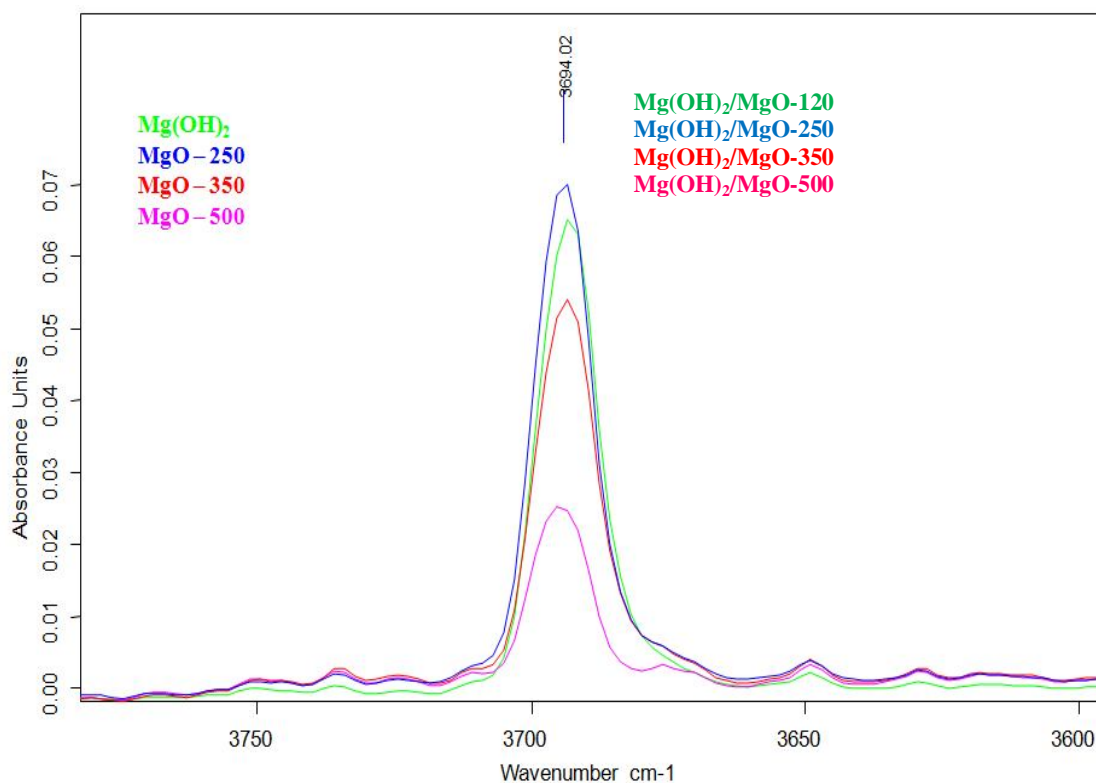


Figure 3. ATR-FTIR spectra of the $\text{Mg}(\text{OH})_2/\text{MgO}$ systems investigated in this work.

Transesterification

Figure 4 shows the $^1\text{H-NMR}$ spectrum of raw (left) and transesterified (right) Jatropha oil. The various peaks are assigned to the different H atoms in the oil molecule according to the insert in the figure. Upon transesterification, a new singlet peak appears at 3.65 ppm (j-peak) corresponding to the hydrogen atoms of the methoxy group. The appearance of this peak is associated with the disappearance of the h and i signals corresponding to the glycerine protons indicating complete transesterification at 60°C

using KOH as a catalyst (1.2% w/w of methanol) with 6-to-1 methanol-to-oil molar ratio. To eliminate the effect of oil concentration in the analyzed samples, the intensity of the j-peak relative to that of the a-peak (which corresponds to terminal CH_3 groups of FAME or oil molecules) is considered as a measure of the extent of transesterification. The reason why the a-peak was chosen for this purpose is that it is not supposed to undergo any change during preesterification or transesterification reactions.

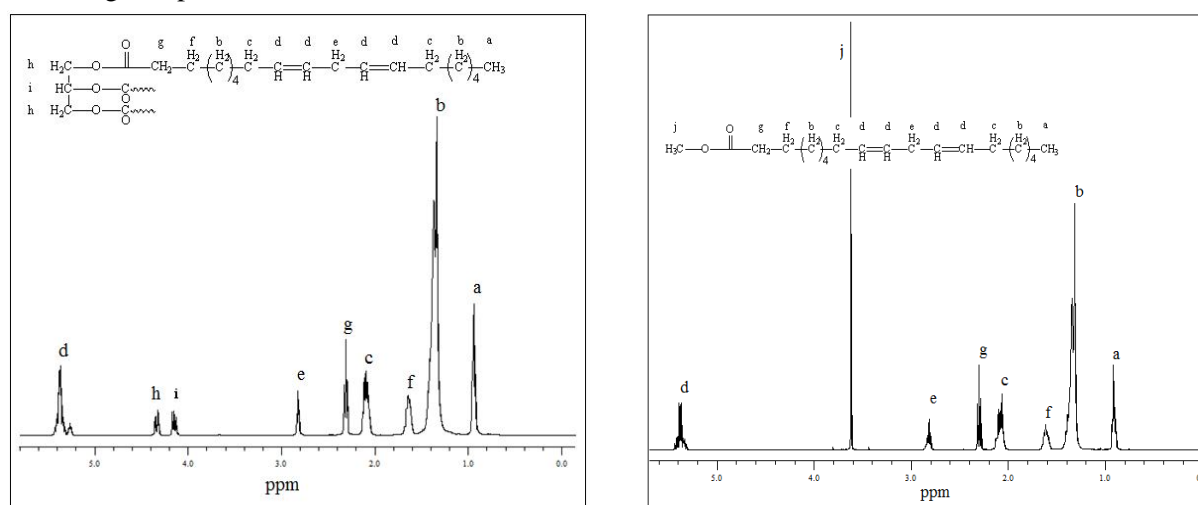


Figure 4. $^1\text{H-NMR}$ spectrum of raw (left) and transesterified (right) Jatropha oil. Transesterification conditions: KOH (1.2% w/w of methanol) and 6:1 methanol/oil molar ratio at 60°C .

The intensity of the j-peak relative to that of the a-peak is shown in Table 1 for raw oil as well as for oil that underwent various preesterification and transesterification processes. Although $\text{Mg}(\text{OH})_2$ (0.0125 g / 1g preesterified oil; 4.35×10^{-4} mol OH^- / g oil) is present in the reaction mixture in larger amounts than KOH (0.0035 g / 1g preesterified oil; 6.24×10^{-5} mol OH^- / g oil), its catalytic performance (17%) is much weaker than that of KOH (96%), obviously due to its limited solubility in methanol. Thermal treatment at 250°C didn't enhance the catalytic behavior of the $\text{Mg}(\text{OH})_2/\text{MgO}$ system, but that at 350°C and 500°C did (72% and 45%, respectively, Table 1). This is very interesting, since the amount of hydroxide groups in $\text{Mg}(\text{OH})_2/\text{MgO}$ -500 for example is much less than in $\text{Mg}(\text{OH})_2$, which suggests that the enhanced behavior of $\text{Mg}(\text{OH})_2/\text{MgO}$ -500 over $\text{Mg}(\text{OH})_2$ results from the MgO component of the system. Obviously, the basic centers on the surface play a significant role as heterogeneous catalytic sites. On the other hand, the performance of $\text{Mg}(\text{OH})_2/\text{MgO}$ -350 (72%) is better than that of $\text{Mg}(\text{OH})_2/\text{MgO}$ -

500 (45%) despite the fact that $\text{Mg}(\text{OH})_2/\text{MgO}$ -500 contains an equal amount of surface basic sites as $\text{Mg}(\text{OH})_2/\text{MgO}$ -350. The higher activity of $\text{Mg}(\text{OH})_2/\text{MgO}$ -350 may be attributed to the higher basic strength of this system compared to that of $\text{Mg}(\text{OH})_2/\text{MgO}$ -500. Another possibility may however lie in the higher solubility of the hydroxide phase in methanol. To clarify this issue, the solubility of $\text{Mg}(\text{OH})_2/\text{MgO}$ -350 and $\text{Mg}(\text{OH})_2/\text{MgO}$ -500 in methanol was determined and found to be 1.53×10^{-4} M and 6.7×10^{-5} M, respectively. Higher solubility means higher hydroxide ion concentrations in methanol which are responsible for the homogeneous catalysis of the transesterification reaction. The total activity of the $\text{Mg}(\text{OH})_2/\text{MgO}$ system is thus a combination of a homogeneous action by dissolved hydroxide ions and a heterogeneous action by the basic surface sites at the surface. Although $\text{Mg}(\text{OH})_2/\text{MgO}$ -500 shows a lower activity than $\text{Mg}(\text{OH})_2/\text{MgO}$ -350, it is better in terms of heterogeneity and thus recyclability, but higher amounts must be used for longer periods of time in order to achieve higher yields.

Table 1. The intensity of the j-peak relative to that of the a-peak.

Description	I_j/I_a	Performance Relative to KOH%
Raw oil	0	0
Preesterification with H_2SO_4^a	0.15	15.6
Transesterification with KOH ^b	0.96	100
Transesterification with $\text{Mg}(\text{OH})_2^c$	0.17	17.7
Transesterification with $\text{Mg}(\text{OH})_2/\text{MgO}$ -250 ^c	0.16	16.7
Transesterification with $\text{Mg}(\text{OH})_2/\text{MgO}$ -350 ^c	0.72	75.0
Transesterification with $\text{Mg}(\text{OH})_2/\text{MgO}$ -500 ^c	0.45	46.9
Extractive transesterification with H_2SO_4^d	0.96	100
Extractive transesterification with $\text{Mg}(\text{OH})_2/\text{MgO}$ -350 ^d	0.48	50.0

a: Oil preesterified with H_2SO_4 .

b: Oil transesterified with KOH.

c: Oil transesterified with different $\text{Mg}(\text{OH})_2/\text{MgO}$ systems.

d: One-step reaction.

Extractive Transesterification

In this method, both extraction of the oil from the seeds and its subsequent transesterification are carried out simultaneously in one step. Extractive transesterification was conducted using H_2SO_4 , KOH and MgO -350 (4 g catalyst / 20 g *Jatropha* for 15 hours at 60°C) as catalysts.

The resulting extract was found to consist of *Jatropha* oil, transesterified oil (FAME), glycerin and methanol, in addition to the homogeneous catalyst used. The organic layer consists of unreacted oil and transesterified oil; its total mass represents the mass of oil extracted from

the seeds and is thus a measure of the extraction efficiency. The degree of subsequent transesterification is given by the $^1\text{H-NMR}$ analysis, as explained above. When H_2SO_4 was used with methanol as the solvent, the extraction power of the process was found to be almost equal to that of hexane. Moreover, the conversion was also almost identical with that achieved in the two-step homogeneous process (95%). On the other hand, using $\text{Mg}(\text{OH})_2/\text{MgO-350}$ as a catalyst leads to the extraction of only 25% of the oil, of which only 50% was tranesterified. Poor extraction efficiency was also observed in the case of KOH (~20%). The above results indicate clearly that the presence of high amounts of sulfuric acid increases significantly the extraction power of methanol, in agreement with the experimental findings reported by other groups^[21]. The use of such rather high amounts of sulfuric acid is however undesired because of its negative impact on the environment.

Biodiesel Analysis

One of the most important diesel characteristics is the cetane number (CN), which is a measure of the fuel's ignition delay; i.e., the time period between the start of injection and the first identifiable pressure increase during combustion of the fuel. In a particular diesel engine, higher cetane fuels will have shorter ignition delay periods than lower cetane fuels. The cetane number (CN) indicates thus how well a fuel will combust inside a compression engine. Biodiesel usually has a higher cetane number than petroleum diesel. The CN of biodiesel varies from 45 to 67^[22]. Usually, the cetane number of the diesel fuel is determined by combusting the sample in specific diesel engines designed for this purpose. Since this is not available here in Jordan, the cetane number was determined through calculations according to the following equation^[23].

$$CN = 46.3 + \left(\frac{5458}{SV}\right) - (0.225 * IN)$$

where CN is the cetane number, SV is the saponification value and IN is the iodine number. This equation is however applicable only for methyl esters.^[21] The cetane number of obtained transesterified oil was calculated to be ~51, which is in accordance with the required ASTM specifications.

Further characteristics of the obtained transesterified oil can be found in Table 2. The flash point of a volatile liquid is the lowest temperature at which it can vaporize to form an ignitable mixture in air. The flash point measured for the produced *Jatropha* biodiesel is at the lower acceptable limit. It is however believed that the flash point is a little bit lowered by the presence of some methanol in the biodiesel that wasn't thoroughly cleaned off. The copper corrosion test serves as a measure of the possible difficulties with copper, brass or bronze parts of the combustion system due to the presence of sulfur compounds in the fuel. The results are rated by comparing the stains on a copper strip to a color-match scale from 1-4. For biodiesel, the copper strip corrosion test value should be as low as 1. High copper strip corrosion indicates a severely degraded or acid-contaminated fuel.

The value of sulfated ash reported for *Jatropha* biodiesel is rather high. This is a little bit surprising, because high values of sulfated ash of biodiesel do usually come from the fuel additives. High values of sulfated ash may however result in the case of having rather high phosphorous content in the oil (as phospholipids). The determination of phosphorous content in biodiesel couldn't be performed due to the lack of necessary chemicals. It is also possible that in the extraction process of oil from the *Jatropha* fruit, some "gum" passes through the filter paper with the oil, leading to the presence of "residuals" in biodiesel. In all cases, this issue needs further attention.

Table 2. Some characteristics of produced Jatropha biodiesel and comparison with ASTM standards.

Test Type	Results	ASTM specifications
Cetane number	51	45-67
Flash point (°C)	93	93 min.
Kinematic viscosity @ 40°C (cSt)	5.7	1.9 – 6
Sulfated ash (%wt)	0.09	0.02 max.
Copper corrosion, 3hrs @ 50°C	1a	1
Saponification value (mg KOH/g oil)	187.66	-
Acidity as oleic acid	0.40%	< 0.5%
Iodine number (g I ₂ / 100 g oil)	108.7	120 max.
Cloud point (°C)	7	-
Distillation @ 90% (°C)	353.3	360 max.

Conclusions

In this work, a series of magnesium oxide-hydroxide catalysts, prepared by precipitation and subjected to thermal treatment at various temperatures, was tested as potential solid catalysts for biodiesel production from Jordanian Jatropha oil. The oil, constituting around 20% of the seed weight, was extracted from the Jatropha seeds using n-hexane as a solvent. The extracted oil has a rather low acid value of 0.86 mg KOH / g Oil corresponding to free fatty acid content (FFA) less than 0.5%. Preesterification with methanol in the presence of H₂SO₄ reduced the acid value further down to 0.73 mg KOH / g Oil.

Thermal treatment was found to play a crucial role in determining the catalytic activity and calcination of Mg(OH)₂ for two hours at 350°C was found to give mixed Mg(OH)₂ and MgO phases with high activity, as rather small amounts of this catalyst (only 0.25 g per 20 g oil) could achieve in three hours of transesterification with methanol at 60°C a conversion of 75%.

The solubility of the above system in methanol was determined to be 1.53×10^{-4} M, suggesting that its catalytic action is both of

homogenous (dissolved hydroxide ions) as well as of heterogeneous (basic surface sites) nature.

Thermal treatment at 500°C results in a less active system (biodiesel yield 47%), which could be related to decreased amount of soluble fraction (solubility in methanol 6.7×10^{-5} M) and to decreased strength of basic surface sites as suggested by the CO₂ desorption experiments. Nevertheless, the system resulting from the thermal treatment at 500°C is believed to be the better one in terms of heterogeneity and thus recyclability; higher amounts must however be used for longer periods of time in order to achieve higher yields,

The specifications of the biodiesel produced in this work match the standards. Sulfated ash is a little bit high, but this was attributed to the poor filtration of the oil before sending it to transesterification.

Acknowledgement

The authors acknowledge the generous funding of the project by the Deanship of Higher Studies and Scientific Research at Yarmouk University.

References

- [1] IRENA (International Renewable Energy Agency), **2014**. Global Bioenergy: Supply and Demand Projections. www.irena.org.
- [2] Helwani, Z.; Othman, M. R.; Aziz, N.; Fernando, W. J. N.; Kim, J. *Fuel Processing Technology*, **2009**, *90*, 1502–1514.
- [3] Correia, L. M.; Campelo, N. D. S.; Novaes, D. S.; Cavalcante Jr., C. L.; Cecilia, J. A.; Rodríguez-Castellón, E.; Vieira, R. S. *Chem. Eng. J.*, **2015**, *269*, 35–43.
- [4] Gupta, J.; Agarwal, M.; Dalai, A. K. *Biocatal. Agricul. Biotechnol.*, **2016**, *8*, 51–59.
- [5] Gutiérrez, Ch. D. B.; Serna, D. L. R.; Alzate, C. A. C. *Biofuel Research Journal*, **2017**, *15*, 691–703.
- [6] Kawashima, A.; Matsubara, K.; Honda, K. *Bioresour. Technol.*, **2008**, *99*, 3439–3443.
- [7] Moncada, J.; El-Halwagi, M. M.; Cardona, C. A. *Bioresour. Technol.*, **2013**, *135*, 533–543.
- [8] Advanced Biofuel Center. <http://www.jatropha-world.org>.
- [9] Wood, P. *Refocus*, **2005**, (July/August), 40–44.
- [10] Hussan, S.; Jamjum, K. Annual reports (in Arabic) on "Energy Production by Cultivating the Jatropha Bushes at Different Environments in Jordan", National Center for Agricultural Research and Extension (NCARE), Baqa', Jordan, **2009**.
- [11] Diserio, M.; Tesser, R.; Pengmei, L., *Energy Fuel*, **2008**, *22*, 207–217.
- [12] Wen, Z.; Yu, X.; Tu, S.; Yan, J.; Dahlquist, E. *Appl Energy*, **2010**, *87*, 743–748.
- [13] Wen, Z.; Yu, X.; Tu, S.; Yan, J.; Dahlquist, E. *Bioresour. Technol.*, **2010**, *101*, 9570–6.
- [14] Lu, F.; Yu, W.; Yu, X.; Tu, S. *Energy Procedia*, **2015**, *75*, 72 – 77.
- [15] Almerindo, G. I.; Probst, L. F. D.; Campos, C. E. M.; de Almeida, R. M.; Meneghetti, S. M. P.; Meneghetti, M. R.; Clacens, J. M.; Fajardo, H. V. *Journal of Power Sources*, **2011**, *196*, 8057– 8063.
- [16] Buasria, A.; Rochanakita, K.; Wongvitvichota, W.; Masa-arda, U.; Loryuenyonga, V. *Energy Procedia*, **2015**, *79*, 562 – 566.
- [17] Yacob, A. R.; Amat Mustajab, M. K. A.; Samadi, N. S., *World Academy of Science, Engineering and Technology*, **2009**, *56*, 408–412.
- [18] Al Qudah, Y.; Telfah, H.; Hammoudeh, A.; Mahmoud, S., *JSM Biotechnol Bioeng*, **2018**, *5* (1), 1083.
- [19] IUPAC, *Standard Methods for the Analysis of Oils, Fats and Derivatives*, 6th Edition, Pergamon, **1979**.
- [20] Bensitel, M.; Moraver, V.; Lamotte, J.; Saur, O.; Lavalley, J. C. *Spectrochim. Acta*, **1987**, *43 A*, 1487–1491.
- [21] Shuit, S. H.; Lee, K. T.; Kamaruddin, A. H.; Yusup, S. *Environ. Sci. Technol.* **2010**, *44*, 4361–4367.
- [22] Nelson, L.; Foglia, T.; Marmer, W. J. *Amer. Oil Chem. Soc.* **1996**, *73*, 1191–5.
- [23] Krisnangkura, K., *J. Amer. Oil Chem. Soc.* **1986**, *3*, 552–3.